IEEE Photonics Journal
An IEEE Photonics Society Publication

Open Access

Hollow Core Antiresonant Fiber With Radially Asymmetric Nodeless Claddings

Volume 10, Number 1, February 2018

Tao-Ying Yu
Xuesong Liu
Zhong-Wei Fan

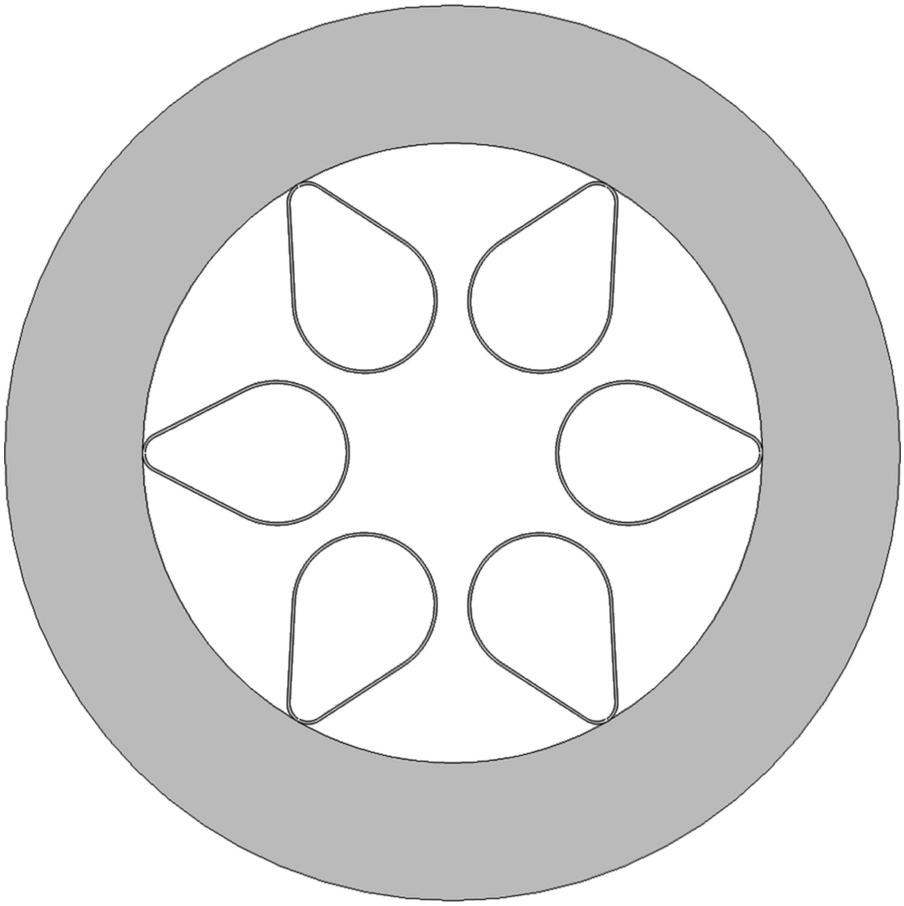

DOI: 10.1109/JPHOT.2017.2786478
1943-0655 © 2017 IEEE

IEEE photonics SOCIETY

IEEE

Hollow Core Antiresonant Fiber With Radially Asymmetric Nodeless Claddings

Tao-Ying Yu,[1, 2, 3] **Xuesong Liu**[1, 2, 4] **and Zhong-Wei Fan**[1, 2, 4]

[1]Academy of Opto-Electronics, Chinese Academy of Science, Beijing 100094, China
[2]National Engineering Research Center for DPSSL, Beijing 100094, China
[3]University of Chinese Academy of Sciences, Beijing 100049, China
[4]Sino-HG Applied Laser Technology Institute Company, Ltd, Tianjin 300304, China

DOI:10.1109/JPHOT.2017.2786478
1943-0655 © 2016 IEEE. Personal use is permitted, but republication/redistribution requires IEEE permission. See http://www.ieee.org/publications standards/publications/rights/index.html for more information.

Manuscript received September 15, 2017; revised November 20, 2017; accepted December 19, 2017. Date of publication December 27, 2017; date of current version January 12, 2018. This work was supported in part by the National Natural Science Foundation of China under Grant 61605215, in part by the Innovation Program of Academy of Opto-Electronics (AOE) of Chinese Academy of Science (CAS) Program under Grant Y50B14A13Y, and in part by the Chinese Innovative Talent Promotion Plans for Innovation Teams in Priority Fields under Grant 2014RA4051. Corresponding authors: Xuesong Liu and Zhongwei Fan (e-mail: b52sjtu@hotmail.com; Fanzhongwei@aoe.ac.cn).

Abstract: We propose and numerically study a novel type of hollow core antiresonant fiber with a single layer of nodeless radially asymmetric cladding tubes, i.e., the cladding tube presents a bulb-like shape, that the local cladding curvature radius at the core/cladding boundary is larger than the other side. Compared with counterparts with conventionally used radially symmetric nodeless claddings, e.g., circular and elliptical tubes, numerical analysis shows that such structure can provide excellent broadband low-loss property and robust single-mode guidance. By tuning the local cladding tube curvature radius, the confinement loss characteristic can be less sensitive but the phase matching between core high-order modes (HOMs) and resonant cladding modes can be significantly enhanced than that of the elliptical structure. Since the cladding modal fields are moved closer to those of the core HOMs, the HOM extinction ratio can reach above 10^4 and maintain over an octave of bandwidth.

Index Terms: Waveguides, fiber optics systems, modeling.

1. Introduction

Recently, hollow core antiresonant fiber (HC-ARF) that guides light via inhibit coupling between core and cladding modes have attracted a great deal of interest, for their ability to guide light in filled gas with significantly lower dispersion and nonlinearity, but much higher damage threshold than the solid-core fibers. HC-ARF is very useful for high-power and large-energy pulsed laser delivery, pulse compression, supercontinuum generation, high-harmonic generation, etc. [1]–[4]. Over the last few years, several types of HC-ARFs with different cladding styles have been studied. The first style is the Kagome fiber, with complex cladding structure composed of multiple layers of small tubes [5], [6]. Very recently, a new class with simple cladding structure consisting of a single ring of cladding tubes is intensively investigated, for it is easier to be fabricated than Kagome-PCF [7], [8].

The transmission loss has always been the most concerned subject for the HC-ARF design engineering, including further lowering the loss level, broadening the transmission bandwidth and extending the transmission capacity to shorter or longer wavelength regions that exclude the solid-core fibers made of fused silica. In the near-IR region, i.e., 1$\sim$2 μm, which covers most doped-fiber

lasing wavelengths, the confinement loss (CL) dominates the loss mechanism [9]. Since HC-ARFs with one layer of touched cladding tubes were proposed but exhibited relatively high CL, a variety of derivative designs have been studied for reducing the CL level, such as the nodeless cladding structure [10], [11], the nested cladding structure [12]–[14]. Besides circular tubes, a single layer of or nested elliptical cladding tubes has also been proposed recently [15], [16].

On the other hand, since the fiber core of interest is as large as tens of micrometers, HC-ARF inherently supports a family of high-order modes (HOMs) in core, which can be excited by slightly bending or external stress on the HC-ARF, and then the output beam quality will be degraded. So HOM suppression comes to be another important research field on HC-ARF [16]–[19]. So far, the efficient way is to increase the HOM losses as high as possible to enhance the HOM extinction ratio (HOMER), defined as the ratio of the lowest loss (in dB/m) of considered HOMs to the fundamental mode (FM) loss. In principle, it is realized by inducing resonant coupling, i.e., phase matching between the core HOMs and the neighboring cladding modes. [17] claims that the size of cladding tubes comparable to that of fiber core is necessary to obtain the phase matching, which is impossible for the Kagome with cladding of small holes. [18] reports a deep theoretical analysis and discloses that for the HC-ARF with a single layer of nodeless circular cladding tubes, there is an optimal radius ratio of the cladding tube to the core, at which the HOMER can reaches 10^3 in principle. This rule is very meaningful for guiding the HC-ARF design aiming to HOM suppression, regardless of a specific core size. However, the CL level for such a standard structure is relatively high.

So far, most reported nodeless cladding structures consist of radially symmetric elements, e.g., circular or elliptical tubes, probably limited by current fiber fabrication technologies. Though the early-emerged HC-ARF with extraordinary cladding structure, i.e., the “ice-cream-cone” cladding behaves well in practice [1], [7], the tube-touched design limits the loss level in principle. In this work, we propose a nodeless HC-ARF design with a single layer of radially asymmetric cladding tubes. In the fiber radial direction, two ends of an individual tube differ from each other. The local curvature radius close to the core is obviously larger than the other side, so that the tube resembles a bulb. Numerical simulations and theoretical analysis demonstrate such a design takes both advantages of the elliptical tube with low CL and the circular tube with high HOMER as in [18]. The calculated CL can be further lowered by several times and less sensitive to geometric variations than the counterpart with elliptical tubes. By tuning the local curvature radius close to the core, the HOMER of the proposed HC-ARF can reach above 10^4, because the resonant cladding modal field distribution is closer to the core HOMs and therefore the phase matching between them is enhanced. Moreover, such improved CL and HOMER performance can be maintained over an octave bandwidth in near-mid-IR wavelength range.

2. Fiber Design

Fig. 1 shows three HC-ARF structures for computational comparison: (a) the regular one with circular cladding tubes, (b) with elliptical cladding tubes and (c) the proposed with radially asymmetric cladding tubes. For a fair comparison, the three structures preserve the same geometric parameters as many as possible: the same thickness of 20 μm for the outer jacket; six equally spaced cladding elements surrounding the hollow core with identical core diameter of 30 μm; the same cladding strut thickness of 0.4 μm. Other parameters are all optimized for the lowest CL values. In Fig. 1(a), the normalized cladding tube diameter with the core diameter, $d/D = 0.65$. In Fig. 1(b), the major axis length of the elliptical tube is 30 μm and the minor semi-axis length is 9.6 μm. The proposed HC-ARF structure with radially asymmetric nodeless claddings is shown in Fig. 1(c): different from a circular/elliptical tube, in the radial direction, two ends are arcs, but the local curvature radius of the tube end at the core/cladding boundary is larger than the other end. In order to reduce the quantitative discussion complexity, the larger tube end is assumed to be a circle with diameter of $d_1 = 0.7D$. The distance between the two tube ends, i.e., the distance from the core to the outer capillary is also 30 μm, the same as the elliptical case in Fig. 2(b).

Although to some extent the proposed HC-ARF looks like the “ice-cream-cone” structure, as shown in Fig. 2(a) in terms of the cladding shape, there are clear distinctions between them. Firstly,

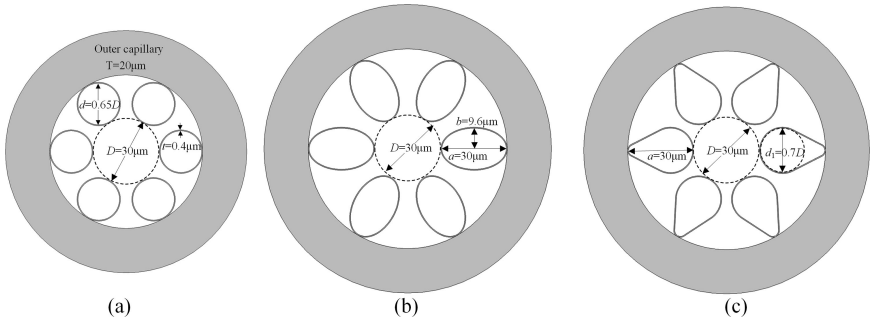

Fig. 1. Three considered nodeless HC-ARF structures for comparison: (a) the regular one with circular cladding tubes, (b) with elliptical cladding tubes and (c) the proposed with radially asymmetric cladding tubes. The three designs share the same parameters of outer capillary thickness, cladding wall thickness and core diameter. The distance from the core to the outer capillary is also kept the same in (b) and (c).

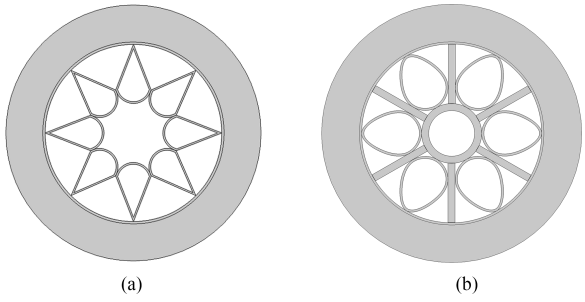

Fig. 2. Diagrams of (a) the HC-ARF with "ice-cream-cone" cladding structure, (b) the preform of proposed HC-ARF with radially asymmetric nodeless claddings, assembly with silica plates inserted between cladding tubes.

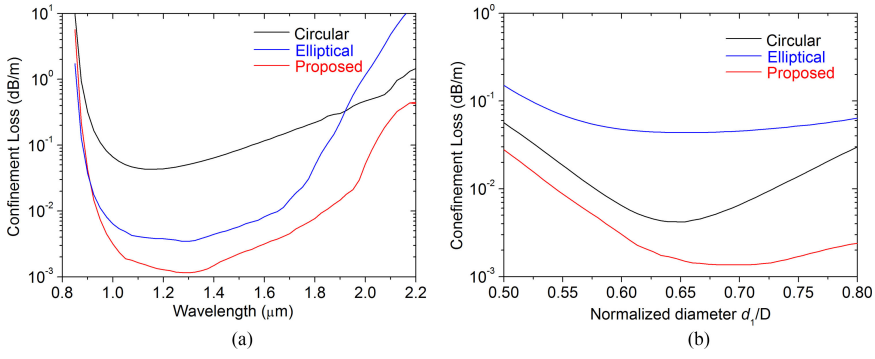

Fig. 3. (a) CL vs. wavelength for the three nodeless HC-ARF structures, i.e., the circular cladding tubes, the elliptical cladding tubes and the proposed radially asymmetric cladding tubes. (b) CL at 1.06 μm wavelength as a function of the normalized local tube diameter for the proposed structures.

the nodeless structure can get rid of the destruction of antiresonant condition and then lower the CL level. Secondly, the cladding tube end at the core/cladding boundary is more circular in our proposed structure, because in the nodeless structure, the surface tension of the cladding tubes tends to eliminate the tear shape. The following will demonstrate that the more approaching to a circular shape, the more core HOM suppression will be achieved. The proposed HC-ARF is possible to be fabricated by the stack and draw technique step by step. The detailed process can be referred to the descriptions in [7] and [14]. The main challenge will be in the second preform fabrication step. As shown in Fig. 2(b), pre-shaped cladding tubes are inserted into a thick capillary with a large diameter as the jacket tube, and are secured with specially produced silica

plate to isolate each cladding tube. Next, precisely adjusting the drawing parameters to balance the gas pressure and the surface tension is the key to control the curvature of the core wall as the elliptical cladding fabrication. It should be noted that the formation of the radial asymmetric cladding concept is far more than the proposed structure in Fig. 1(c), which is only to reduce the discussion complexity here. The arc of the larger cladding end can be a segment of an ellipse or other shapes, or even the whole tube shape can be depicted by a general curve equation. The critical features of the proposed HC-ARF designs are: i) the tube dimension is larger in the radial direction than in the azimuthal direction; ii) the local curvature radius at the core/cladding boundary is larger than the other side; iii) the tubes do not touch each other.

3. Confinement Loss

The numerical simulation is performed based on the full-vectorial-finite-element method along with anisotropic perfectly matched layers (PML) on the outer jacket as the boundary condition. Attributed to the PML boundary condition, the calculation results can be independent on the outer jacket thickness. In the calculation, the fiber material dispersion is considered, and hence the results may differ from those keeping the refractive index (RI) as a constant. The RI of the fused silica is given by the Sellmeier equation [20],

$$n(\lambda) = \sqrt{1 + \sum_{i=1}^{3} \frac{B_i \lambda^2}{\lambda^2 - C_i}}, \tag{1}$$

Where the Sellmeier coefficient B_i equals to 0.6961663, 0.4079426 and 0.8974794, and C_i equals to $4.67914826 \times 10^{-3}\,\mu\text{m}^2$, $1.35120631 \times 10^{-2}\,\mu\text{m}^2$, and $97.9340025\,\mu\text{m}^2$, respectively. From the "ARROW" model [21], the high-loss inhibited band wavelengths in the transmission spectrum are determined by $\lambda_{res} = 2t\sqrt{n^2 - 1}/m$, where t is the cladding strut thickness, and m is a positive integer. Then the wavelength of the first resonant loss peak is around 0.84 μm.

Fig. 3(a) demonstrates the calculated CL spectra for the three optimized nodeless HC-ARF designs, as shown in Fig. 1. In the short wavelength region, the three CL curves tend to be high near 0.84 μm, as predicted by the ARROW model. For the circular cladding tube case, the minimum CL value is 40 dB/km at 1.15 μm, while the lowest CL for the elliptical cladding case is 3.9 dB/km at 1.3 μm, an order magnitude lower than the former. The CL improvement for the latter mainly attributes to the larger radial distance from the core to the outer capillary, which is impossible for the former, or else the circular cladding tubes will touch or overlap each other if its diameter takes the same length as the major axis of an ellipse. Such distance is negatively correlative to the CL level. This rule is reasonable by considering that the isolated hollow capillary, where the equivalent distance is zero, has the smallest mode confinement effect, or in other words, the largest CL level. However, the CL values for the elliptical case increases rapidly at long wavelength region, and becomes larger than the circular case from 1.9 μm. This means the modal coupling increases between the core FM and the localized mode in the cladding struts. For the proposed radially asymmetric case, the lowest CL value is only 1.1 dB/km at 1.3 μm, three times smaller than the elliptical case. It can be seen that the transmission band is very broad in the near-IR region. And the CL curve is lower than the two counterparts throughout the considered wavelength span, from 0.85 to 2.2 μm. Firstly, the proposed structure has the advantage as the elliptical case, that the distance from the core to the outer capillary is elongated in the radial direction [16]. Secondly, compared with the elliptical case, the further improvement of the CL property, attributes to larger local tube size close to the core, meaning smaller cladding tube gaps, so less FM field leaks from the gaps and then the FM confinement is enhanced. In contrast, for an elliptical tube, the convex part is in the middle. Fig. 3(b) shows the CL as a function of the normalized cladding tube diameter, i.e., d/D for the circular case, $2b/D$ for the elliptical case and d_1/D for the proposed case. The wavelength is fixed at 1.06 μm, in terms of Yb-based fiber laser applications. As shown in Fig. 3(b), each CL curve has an optimum normalized diameter for the lowest CL value. However, the curves of the circular case and the proposed case are more flat than the elliptical case as $d_1/D > 0.65$. From a

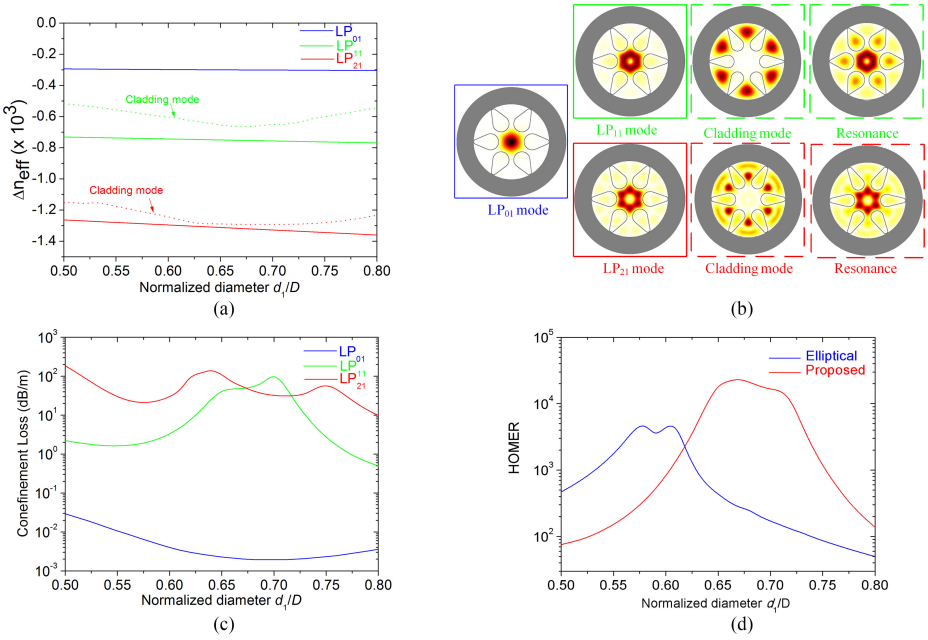

Fig. 4. (a) Relative ERIs, (b) FM and HOMs' modal field profiles, (c) CL and (d) HOMER (the proposed case and the elliptical cladding case) vs. normalized local tube diameter at 1.06 μm wavelength. Noted that the higher modal field intensities in the cladding and core simultaneously, the higher resonant coupling and hence the higher HOMER.

practical viewpoint, flat curve distribution is in favor of fabrication tolerance on the cladding tube. In other words, d_1/D can be varied in a broader range to achieve a low CL level for the circular and the proposed HC-ARF designs.

4. High-order Mode Suppression

The task of HOM suppression is to increase HOM losses as high as possible while to maintain low FM loss through fiber design engineering. The mechanism is resonant modal couplings between core HOMs and neighboring cladding modes. Such modal coupling usually occurs when a HOM undergoes a strong anti-crossing with a cladding tube mode, embodied as effective RIs (ERIs) of the two modes approaching each other. Here, the core modes and the cladding tube modes are respectively noted as LP_{lm} and ARE_{lm}, where l and m indicate the azimuthal and radial orders of the mode. The modal ERIs in a capillary can be roughly estimated by the Marcatili-Schmeltzer expression [22]

$$n_{lm} = \sqrt{n_{air}^2 - \frac{u_{lm}^2}{(k_0 d/2)^2}}, \tag{2}$$

where, n_{air} is the air RI in atmosphere; u_{lm} is the m-th root of the Bessel function J_l; k_0 is the wave number in vacuum and d here is the capillary diameter. Take the first core HOM, LP_{11} for instance, supposing the core and cladding tubes are all circular, when the diameter ratio is $d/D \approx 0.63$, basically agreeing with the result in [12], then $n_{LP_{11}} \approx n_{ARE_{01}}$, indicating the LP_{11} mode is resonant with ARE_{01} mode, so that the largest HOMER for LP_{11} mode is realized.

In our calculation, the FM, LP_{01} mode and the first two core HOMs, LP_{11} and LP_{21} modes are considered. Though for a comprehensive analysis, all the HOMs should be considered, FEM shows other higher-order modes always exhibit much high CL, indicating they have insignificant impact on the single-mode performance, and in experiment they are also difficult to be excited. Fig. 4(a) shows the relative ERI, $\Delta n_{eff} = n_{eff} - 1$ of the core modes and the resonant cladding modes,

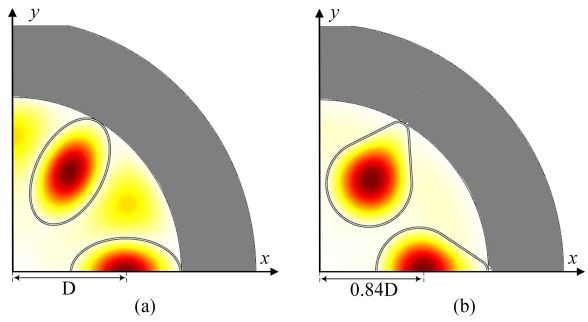

Fig. 5. ARE_{01} modal field distributions in (a) the elliptical cladding tubes and in (b) the radially asymmetric cladding tubes.

as functions of the normalized cladding tube diameter d_1/D. Fig. 4(b) plots the modal field profiles in different modal coupling situations. Fig. 4(c) plots the core-mode-CL curves versus d_1/D. In Fig. 4(a), the LP_{01} mode has the highest Δn_{eff}, which remains almost constant. The Δn_{eff} of the LP_{11} and LP_{21} modes decreases linearly with d_1/D increase. There is no resonant cladding mode for the LP_{01} mode in one transmission band, for the fiber core size is larger than the cladding tube and the gaps between cladding tubes, so the CL is very small. However, for a core HOM with low-ERI, there are possible resonant cladding modes with slightly larger relative ERIs. The phase-matching extent between a core HOM and the neighboring resonant cladding mode determines the core HOM loss. The HOM CL curves shown in Fig. 4(c) can be explained by the Δn_{eff} distributions presented in Fig. 4(a) and the modal field profile variations in Fig. 4(b). For the LP_{11} mode, when d_1/D is small, i.e., the cladding tube size is smaller than the tube gap, the neighboring cladding modes exist inside both the cladding tubes (ARE_{01} mode) and the tube gaps. As shown in Fig. 4(b) (the second column of the upper row), the modal profile diagram, the cladding modes localized in tube gaps are stronger than ARE_{01} mode, and because the gap mode is far from the core, the modal coupling effect with respect to LP_{11} mode is relatively weak. This is evident by the large relative ERI deviation of the LP_{11} mode and ARE_{01} mode in Fig. 4(a). Then the initial CL of the LP_{11} mode is small, as shown in Fig. 4(c). When the cladding tube size gets larger, ARE_{01} mode becomes stronger and thus the phase matching is enhanced, embodied as the relative ERI of the cladding mode approaches the HOM mode, resulting in high CL of the LP_{11} mode and high core HOMER. However, the situation is different for the LP_{21} mode, part of which modal field enters the tube gaps, as shown in the lower row of Fig. 4(b). Hence even when d_1/D is small, the LP_{21} mode can be resonant with the tube gap modes, and then the CL level always remains high. Fig. 4(d) shows the excellent HOM-suppression performance of the proposed HC-ARF, calculated from the data in Fig. 4(c). The HOMER can be maintained larger than 10^4 when d_1/D ranges from 0.65 to 0.72 and reaches the maximum value of 2×10^4 at 0.675, agreeing well with the conclusion in [18]. As a comparison, the HOMER curve of the elliptical cladding case is also shown in Fig. 4(d). It can be seen our proposed structure has more excellent HOMER over the elliptical cladding case, in terms of the maximum HOMER value and the low CL span (refer to Fig. 3(b)). It mainly attributes to two aspects. At first, according to the definition of HOMER, low CL of the core FM inherently favors a larger value of HOMER. At second, circular core/cladding boundary is more advantageous than the elliptical shape. It is not difficult to understand from a geometric sense. For the elliptical cladding tube, because of the radial symmetry, the ARE_{01} modal field center is at the geometric center of an ellipse, distant from the fiber core center by length D (fiber core diameter), as shown in Fig. 5(a). In contrast, for our proposed radially asymmetric cladding tube, the local curvature radius of the end close to the core is obviously larger than the other end, which makes the ARE_{01} modal field center not in the radial middle, but pushed towards to the core direction. As shown in Fig. 5(b), the distance between ARE_{01} modal field center and fiber core center is reduced to $0.84D$. When the local cladding tube is circular, such distance is at the minimum. From the modal coupling theory, the closer two resonant modes, the stronger for the modal coupling. So

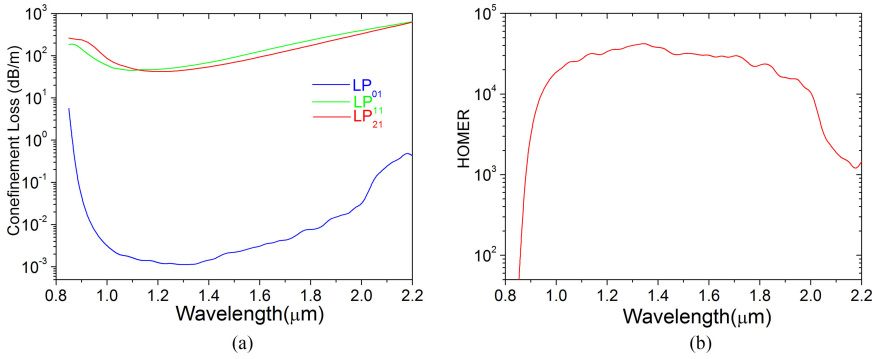

Fig. 6. The optical spectra of the CL (a) and the HOMER (b) of the proposed structure.

our proposed radially asymmetric cladding structure can enhance the phase matching between the core HOMs and resonant cladding modes, and thus increase the HOMER.

Fig. 6(a) and (b) plot the respective CLs of the three core HOMs and the HOMER versus wavelength, when $d_1/D = 0.675$. Because of the large tolerance of d_1/D deviation, as discussed above, the broadband low-CL property of the LP_{01} mode and the high-CL properties of the HOMs remain over an octave of bandwidth. Then the HOMER can be maintained larger than 1×10^4 from 1.0 μm to 2.0 μm. Thus, this proposed HC-ARF can support robust single-mode guidance.

5. Conclusion

In summary, we propose a novel concept of HC-ARF structure. The bulb-like cladding is composed of a single layer of radially asymmetric nodeless tubes. The tube dimension is larger in the radial direction than in the azimuthal direction and the local tube radius close to the core/cladding boundary is larger than the other end. Such cladding tube has both advantages of elliptical tubes with low CL and circular tubes with high HOMER. Numerical analysis shows the CL can be as low as 1.1 dB/km, further lowered than the elliptical case by several times. And the low-loss level is insensitive to geometrical variations, which will increase the fabrication tolerance. By tuning the local cladding tube radius close to the core, the resonant phase matching between core HOMs and cladding modes can be effectively enhanced, for the cladding modal field center is moved closer to the core, and then the HOMER can reach as high as 2×10^4. Moreover, the low-CL and high HOMER properties can be maintained over an octave wavelength bandwidth. This work provides a new design idea to realize a simple-structure HC-ARF with low CL and robust single-mode operation.

Acknowledgment

The authors are very grateful to A. Pryamikov for his useful discussion and suggestions. Translations and content mining are permitted for academic research only.

References

[1] P. Jaworski *et al.*, "High energy green nanosecond and picosecond pulse delivery through a negative curvature fiber for precision micro-machining," *Opt. Exp.*, vol. 23, no. 7, pp. 8498–8506, 2015.
[2] T. Balciunas *et al.*, "A strong-field driver in the single-cycle regime based on self-compression in a kagome fibre," *Nature Commun.*, vol. 6, 2015, Art. no. 6117.
[3] J.-M. Ménard, F. Köttig, and P. St. J. Russell, "Broadband electric-field-induced LP01 and LP02 second harmonic generation in Xe-filled hollow-core PCF," *Opt. Lett.*, vol. 41, no. 16, pp. 3795–3798, 2016.
[4] M. I. Hasan, N. Akhmediev, and W. Chang, "Mid-infrared supercontinuum generation in supercritical xenon-filled hollow-core negative curvature fibers," *Opt. Lett.*, vol. 41, no. 21, pp. 5122–5125, 2016.
[5] N. V. W. Y. Y. Wang, F. Couny, P. J. Roberts, and F. Benabid, "Low loss broadband transmission in hypocycloid-core Kagome hollow-core photonic crystal fiber," *Opt. Lett.*, vol. 36, no. 5, pp. 669–671, 2011.

[6] F. Benabid *et al.*, "Stimulated Raman scattering in hydrogen-filled hollow-core photonic crystal fiber," *Science*, vol. 298, no. 5592, pp. 399–402, 2002.
[7] F. Yu, W. J. Wadsworth, and J. C. Knight, "Low loss silica hollow core fibers for 3–4 μm spectral region," *Opt. Exp.*, vol. 20, no. 10, pp. 11153–11158, 2012.
[8] A. D. Pryamikov *et al.*, "Demonstration of a waveguide regime for a silica hollow-core microstructured optical fiber with a negative curvature of the core boundary in the spectral region$>$3.5 μm," *Opt. Exp.*, vol. 19, no. 2, pp. 1441–1448, 2011.
[9] Y. Fei and J. C. Knight, "Negative curvature hollow-core optical fiber," *IEEE J. Sel. Topics Quantum Electron.*, vol. 22, no. 2, Mar./Apr. 2016, Art. no. 4400610.
[10] A. N. Kolyadin *et al.*, "Light transmission in negative curvature hollow core fiber in extremely high material loss region," *Opt. Exp.*, vol. 21, no. 8, pp. 9514–9519, 2013.
[11] C. Wei, C. R. Menyuk, and J. Hu, "Impact of cladding tubes in chalcogenide negative curvature fibers," *IEEE Photon. J.*, vol. 8, no. 3, Jun. 2016, Art. no. 2200509.
[12] F. Poletti, "Nested antiresonant nodeless hollow core fiber," *Opt. Exp.*, vol. 22, no. 20, pp. 23807–23828, 2014.
[13] M. S. Habib, O. Bang, and M. Bache, "Low-loss hollow-core silica fibers with adjacent nested anti-resonant tubes," *Opt. Exp.*, vol. 23, no. 13, pp. 17394–17406, 2015.
[14] A. F. Kosolapov *et al.*, "Hollow-core revolver fibre with a double-capillary reflective cladding," *Quantum Electron.*, vol. 46, no. 3, pp. 267–270, 2016.
[15] F. C. Meng *et al.*, "Low loss hollow-core antiresonant fiber with nested elliptical cladding elements," *IEEE Photon. J.*, vol. 9, no. 1, Feb. 2017, Art. no. 7100211.
[16] M. S. Habib, O. Bang, and M. Bache, "Low-loss single-mode hollow-core fiber with anisotropic anti-resonant elements," *Opt. Exp.*, vol. 24, no. 8, pp. 8429–8436, 2016.
[17] A. Hartung *et al.*, "Low-loss single-mode guidance in large-core antiresonant hollow-core fibers," *Opt. Lett.*, vol. 40, no. 14, pp. 3432–3435, 2015.
[18] P. Uebel *et al.*, "Broadband robustly single-mode hollow-core PCF by resonant filtering of higher-order modes," *Opt. Lett.*, vol. 41, no. 9, pp. 1961–1964, 2016.
[19] C. Wei *et al.*, "Higher-order mode suppression in chalcogenide negative curvature fibers," *Opt. Exp.*, vol. 23, no. 12, pp. 15824–15832, 2015.
[20] J. W. Fleming, "Dispersion in GeO2–SiO2 glasses," *Appl. Opt.*, vol. 23, no. 24, pp. 4486–4493, Dec. 15, 1984.
[21] N. M. Litchinitser *et al.*, "Antiresonant reflecting photonic crystal optical waveguides," *Opt. Lett.*, vol. 27, no. 18, pp. 1592–1594, 2002.
[22] E. A. J. Marcatili and R. A. Schmeltzer, "Hollow metallic and dielectric waveguides for long distance optical transmission and lasers," *Bell Syst. Tech. J.*, vol. 43, no. 4, pp. 1783–1809, 1964.